IOP Publishing Journal of Geophysics and Engineering
J. Geophys. Eng. 15 (2018) 26–41 (16pp) https://doi.org/10.1088/1742-2140/aa83ca

Paleogeographic evolution of carbonate reservoirs: geological and geophysical analysis at the Albian Campos Basin, Brazil

Maria Gabriela Castillo Vincentelli[1,4], **Julia Favoreto**[2] and **Eduardo Roemers-Oliveira**[3]

[1] FUNDUNESP—Universidade Estadual Paulista, Rio Claro, Brazil
[2] Universidade Federal do Rio de Janeiro, Lagesed, Rio de Janeiro, Brazil
[3] Petrobras, Cenpes, Rio de Janeiro, Brazil

E-mail: g_vicentelli@yahoo.es, juliafavoreto@yahoo.com.br and roemers@petrobras.com.br

Received 30 November 2016, revised 19 June 2017
Accepted for publication 3 August 2017
Published 7 December 2017

Abstract

An integrated geophysical and geological analysis of a carbonate reservoir can offer an effective method to better understand the paleogeographical evolution and distribution of a geological reservoir and non-reservoir facies. Therefore, we propose a better method for obtaining geological facies from geophysical facies, helping to characterize the permo-porous system of this kind of play. The goal is to determine the main geological phases from a specific hydrocarbon producer (Albian Campos Basin, Brazil). The applied method includes the use of a petrographic and qualitative description from the integrated reservoir with seismic interpretation of an attribute map (energy, root mean square, mean amplitude, maximum negative amplitude, etc), all calculated at the Albian level for each of the five identified phases. The studied carbonate reservoir is approximately 6 km long with a main direction of NE–SW, and it was sub-divided as follows (from bottom to top): (1) the first depositional sequence of the bank was composed mainly of packstone, indicating that the local structure adjacent to the main bank is protected from environmental conditions; (2) characterized by the presence of grainstone developed at the higher structure; (3) the main sequence of the peloidal packstone with mudstones oncoids; (4) corresponds to the oil production of carbonate reservoirs formed by oolitic grainstone deposited at the top of the carbonate bank; at this phase, rising sea levels formed channels that connected the open sea shelf with the restricted circulation shelf; and (5) mudstone and wackestone represent the system's flooding phase.

Keywords: carbonate shoal, grainstone, carbonate facies, permo-porous system

(Some figures may appear in colour only in the online journal)

1. Introduction

Nowadays, the main problem associated with carbonate reservoir analysis is the geological/geophysical characterization of its heterogeneous reservoir facies distribution. This implies a high geological complexity, but the objective is the reservoir's composition in terms of its permo-porous system, which depends on an intricate combination of depositional and diagenetic processes.

In this context, the geological characterization of a permo-porous system, when only well data is utilized, could lead to misinterpretations relating to the distribution of these heterogeneities in higher scales than well data (centimeters and meters), as well as seismic scale (tens and hundreds of meters). In order to minimize the upscale error and to better control the data extrapolation related to rock properties along the reservoir, the proposed method uses geological and geophysical analysis based on seismic volumetric interpretation, allowing an indirect visualization of the reservoir's heterogeneities.

[4] Author to whom any correspondence should be addressed.

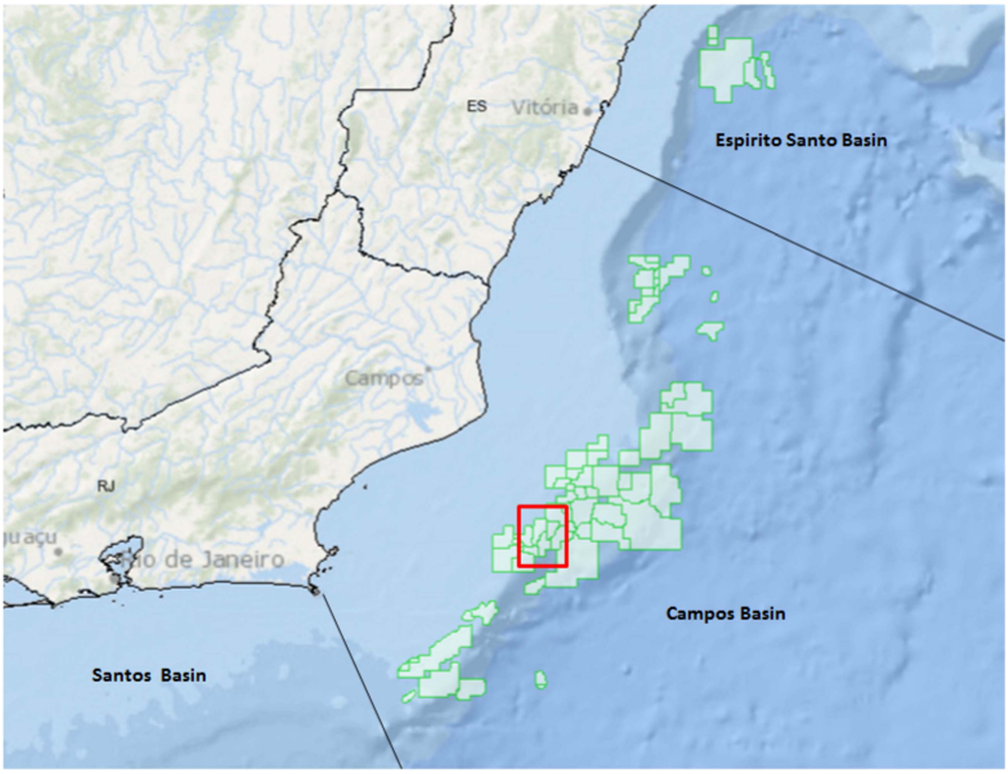

Figure 1. Map of the Campos Basin location showing the main hydrocarbon oil fields. The studied oil field is located inside the red square.

Thus, a combination of rock analysis (core and thin section descriptions) and the evaluation of facies variation using seismic attribute maps tend to lower the uncertainty related to the limited geological and geophysical data; as a result, better control of the reservoir's flow units is expected.

1.1. Objective

The main objective consists of the geophysical and geological characterization of the geological development phases (or depositional sequences) of carbonate field hydrocarbon production at Campos Basin (Brazil). In order to achieve this goal, the depositional facies were characterized using core and petrographic descriptions considering the paleo-environment reservoir's condition. The geological data were integrated with tectonic and sedimentary evolution defined by the surface's seismic attributes created for each bank's development phase, previously defined by a petrographic description (upscaling of the data—micro/meso to macro).

1.2. Study area

The study area corresponds to an oil field in the carbonate bank at the meridional portion of the Campos Basin (offshore region in the east of the Brazilian margin (figure 1)). The Campos Basin extends from the north of Rio de Janeiro State (Cabo Frio High) where it has its boundaries with the Santos Basin, to the state line with Espirito Santo State (Vitoria High) limited to the Espirito Santo Basin.

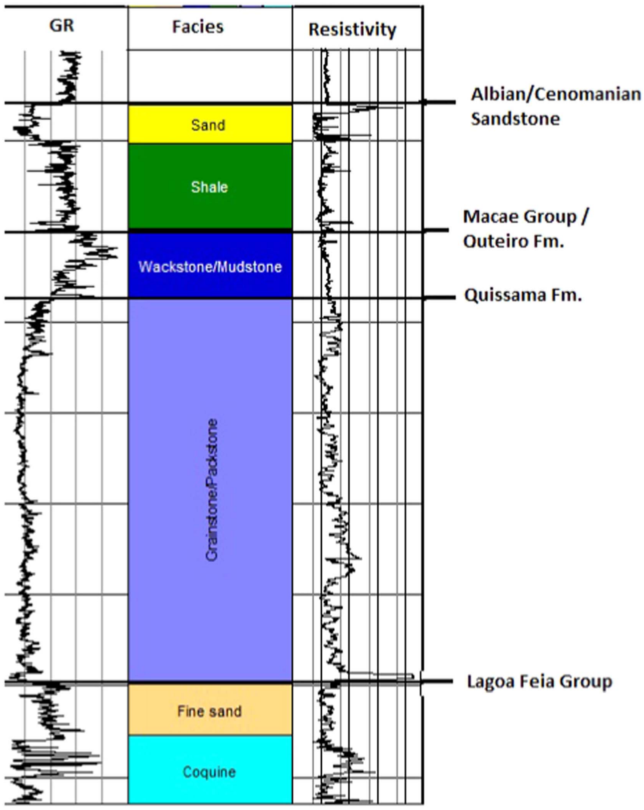

Figure 2. Macae Group facies on a gamma ray and resistivity wirelogs. The Albian/Cenomanian sandstone is equivalent to Namorado formation.

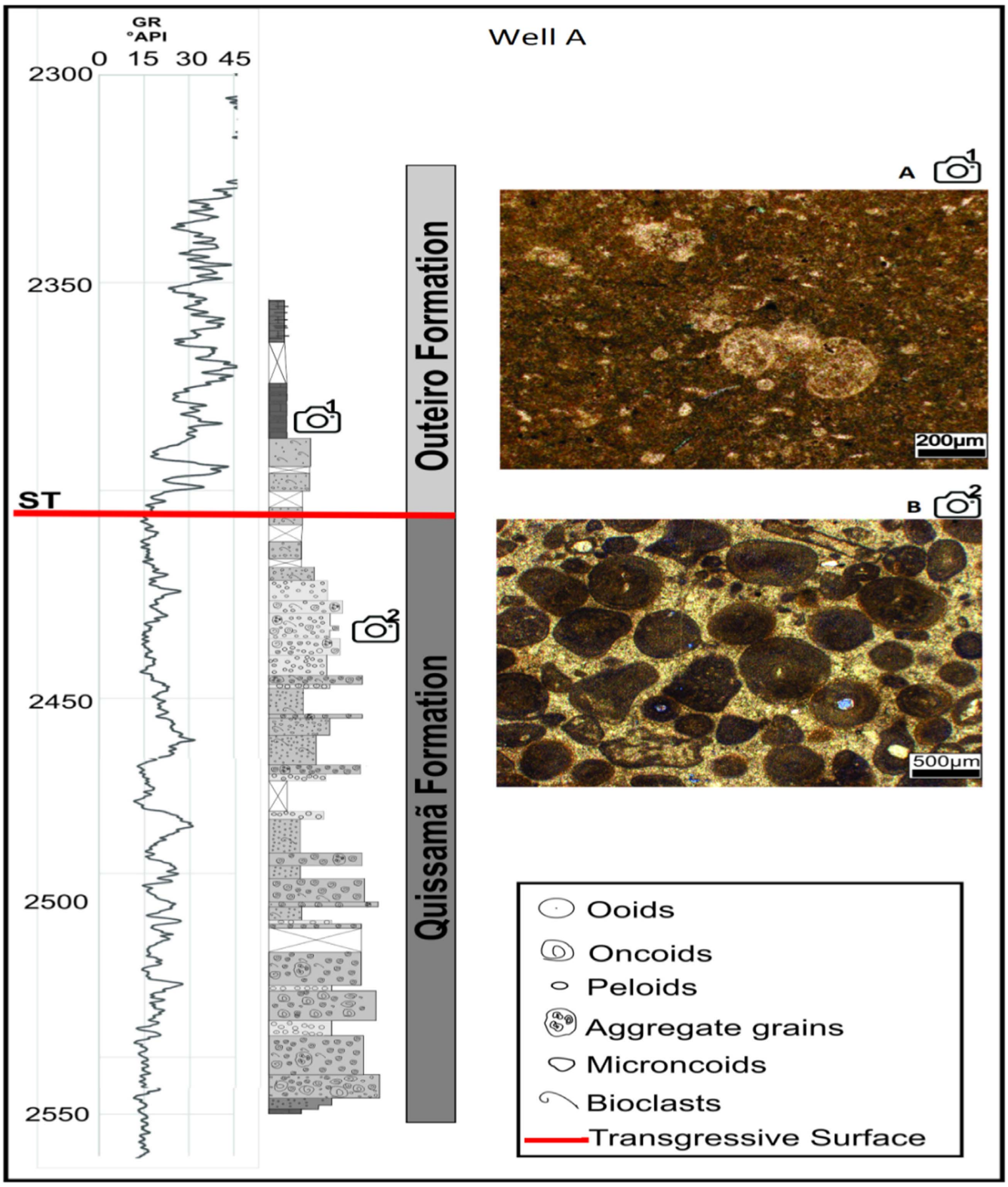

Figure 3. Typical lithological profile for the evaluated oil field. The figure shows a gamma ray profile, a lithologic description of the cores, and thin sections representative of the Outeiro formation and Quissama formation. (A) Mudstone bioclastic/Outeiro formation: micrite matrix with planktonic foraminífera and *Favusella washitensis*—depth 2378.8 m; (B) grainstone oolítico—Quissama formation grain of ooids micritized subspherial and spherical, with partial and high cementation, open structure.

It is important to mention that the Campos Basin is part of the offshore Brazilian basins, approximately 500 km^2, and it is considered that its offshore limit is close to the isobaths of 3400 m.

1.3. Geological context

The tectonic and structural evolution of South America's east margin allowed a continuous system of Mesozoic–Cenozoic basins to develop, created by tectonic processes related to the breakup of Gondwana and the opening of the Atlantic Ocean. The reservoir we studied is related to the Macae Group (figure 2) which is comprised of: (a) Outeiro formation, seal rock, represented by mudstone and wackestone facies; and (b) Macae formation, reservoir rock, described as mainly grainstone facies. Until 2007, the Macae Group was recognized as Macae formation (Rangel *et al* 1994), but, following this theory, it was reviewed by Winter *et al* (2007) and characterized as a group including Goitacas, Quissama, Outeiro, and Namorado formations, as defined by Rangel *et al* (1994), and Imbetiba formation reported by Winter *et al* (2007).

In one of the latest theories relating to the tectonic-sedimentary evolution of the Campos basin, Winter *et al* (2007) defines the basin evolution in three major super sequences: rift, transitional and passive margin—the passive margin (Albian to Quaternary) highlighting the start of the actual marine sedimentation (carbonate at the beginning and mainly siliciclastic sedimentation at the Cenozoic), followed

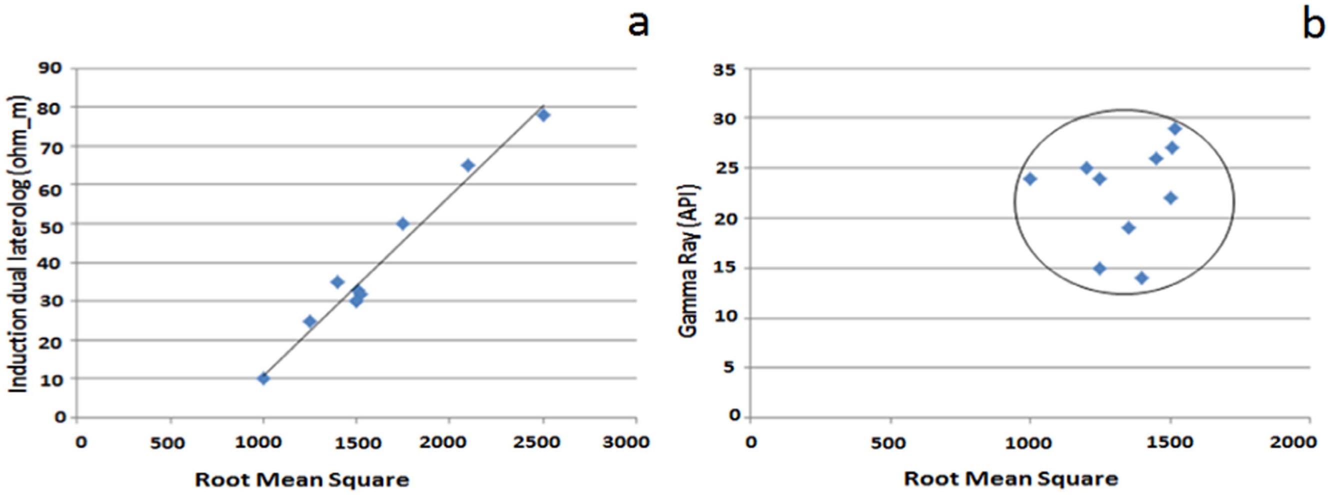

Figure 4. Graphic of cross-correlation of amplitude veruss rock attributes. (A) Linear correlation between seismic and rock attributes. (B) Non correlation between seismic and rock attributes.

Table 1. Geological facies described for the study area (modified after Favoreto *et al* (2016)).

	Facies	Description
Quissama formation	Oolitic grainstone	Medium calcarenite, composed of well sorted ooids (0.3–0.5 mm) with a quartz nucleus. Showing partial to total micritization. Rare bioclasts (fragments of bivalves, echinoids, gastropods, foraminiferas). Two cementation phases: prismatic fringe, which keeps open the framework during eodiagenesis, and mosaic, which obliterates almost all intergranular pores.
	Oncolitic grainstone with ooids	Medium calcarenite, composed of well-rounded and well-sorted oncoids from 0.5–0.7 mm. The nucleus can be composed of echinoids, bivalves, and red algae fragments. Bioclasts of porcelaneous foraminifera. Pores enhanced by dissolution.
	Peloidal packstone with rudaceous oncoids	Calcarenite/calcirudite, very poorly sorted. Oncoids to 2.5 cm. Bioclasts of foraminifera, bivalves and gastropods.
	Peloidal wackestone/packstone	Calcilutite/calcarenite showing a partial dolomitization. Rare gastropods bioclast. Abundance of stilolites.
	Peloidal	Composed of oncoids (0.5 mm), micro-oncoids and peloids (0.1 mm). Echinoids and benthic hyaline foraminifera dispersed within the matrix. Moldic porosity and enhanced pores by dissolution.
	Bioclasts packstone	
	Oncoids	Calcarenite composed of oncoids (0.5 mm), micro-oncoids and peloids (0.1 mm). Echinoids and benthic hyaline foraminifera dispersed. Echinoids bioclasts show syntaxial overgrowth.
	Packstone/grainstone	
Outeiro formation	Peloidal	Peloidal wackestone with pithonelids interbedded by marl.
	Wackestone interbedded by marl	
	Mudstone	Calcilutite mostly composed of micrite, containing pithonelids (*Pithonella sphaerica* and *Pithonella ovalis*) and radiolarians. Benthic and planktonic foraminifera and echinoids fragments are rare. Framboidal pyrites.
	Bioclasts wackestone	Calcilutite, composed of micrite, quartz and glauconite grains with echinoids, red algae and pithonelids bioclasts.

by an intense halo kinetic deformation. This tectonic-sedimentary evolution has been discussed for at least 30 years by many authors, such as Asmus (1975), Asmus and Guazelli (1981), Azevedo *et al* (1987), Guardado *et al* (1989), Dias *et al* (1990), Mohriak *et al* (1990), Chang *et al* (1992), Cainelli and Mohriak (1998), Guardado *et al* (2000), Azevedo (2001), among others.

The Quissama and Outeiro formations at the study area, represent different sea level conditions, although they belong to the same geological period (Albian (figure 3)). Both formations are described as follows:

The Quissama formation is characterized by carbonate banks in the NE-SW direction (Guardado *et al* 1989)

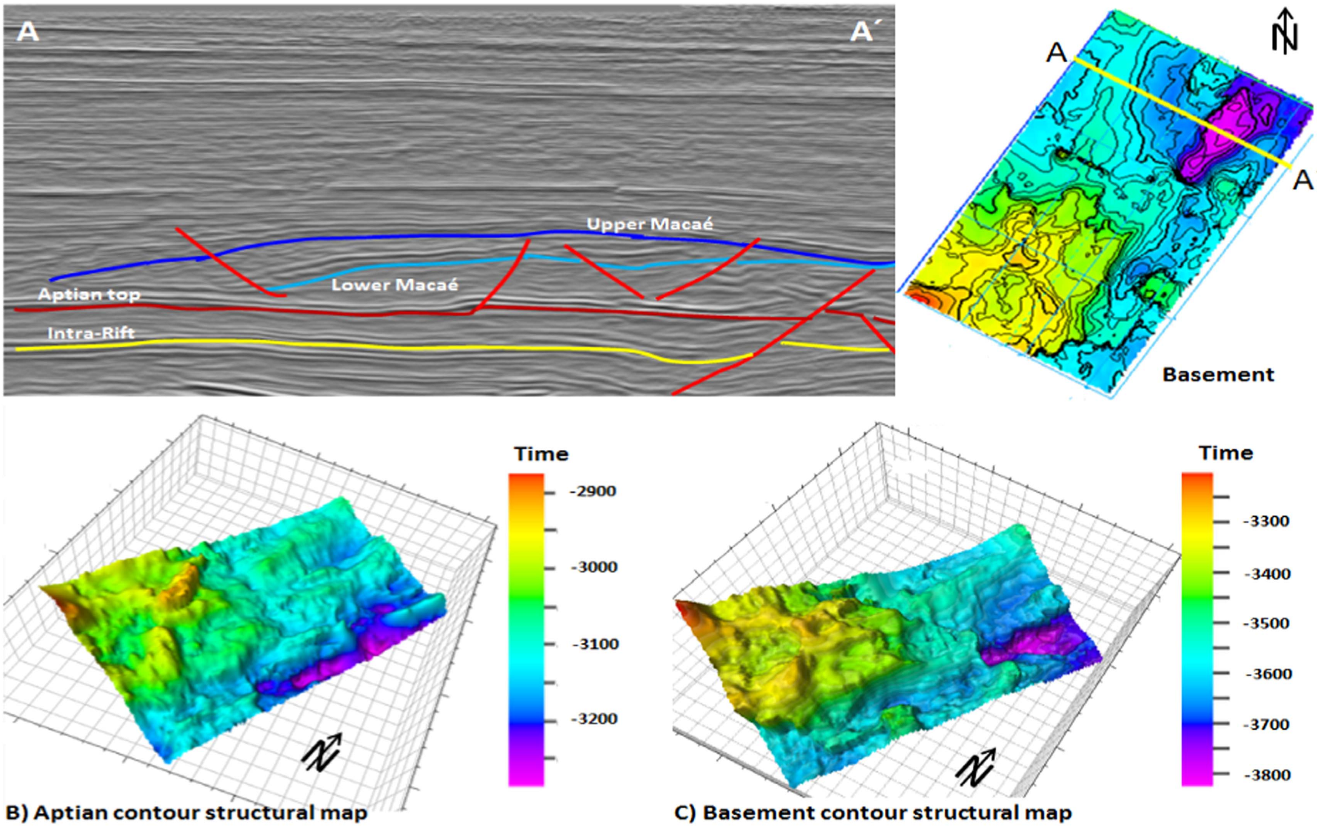

Figure 5. (A) Seismic interpretation and contour structural map of the basement (2D); (B) Aptian structural map in 3D showing the structural paleo-highs in the SW region; (C) basement structural map in 3D showing the structural paleo-highs in the SW region.

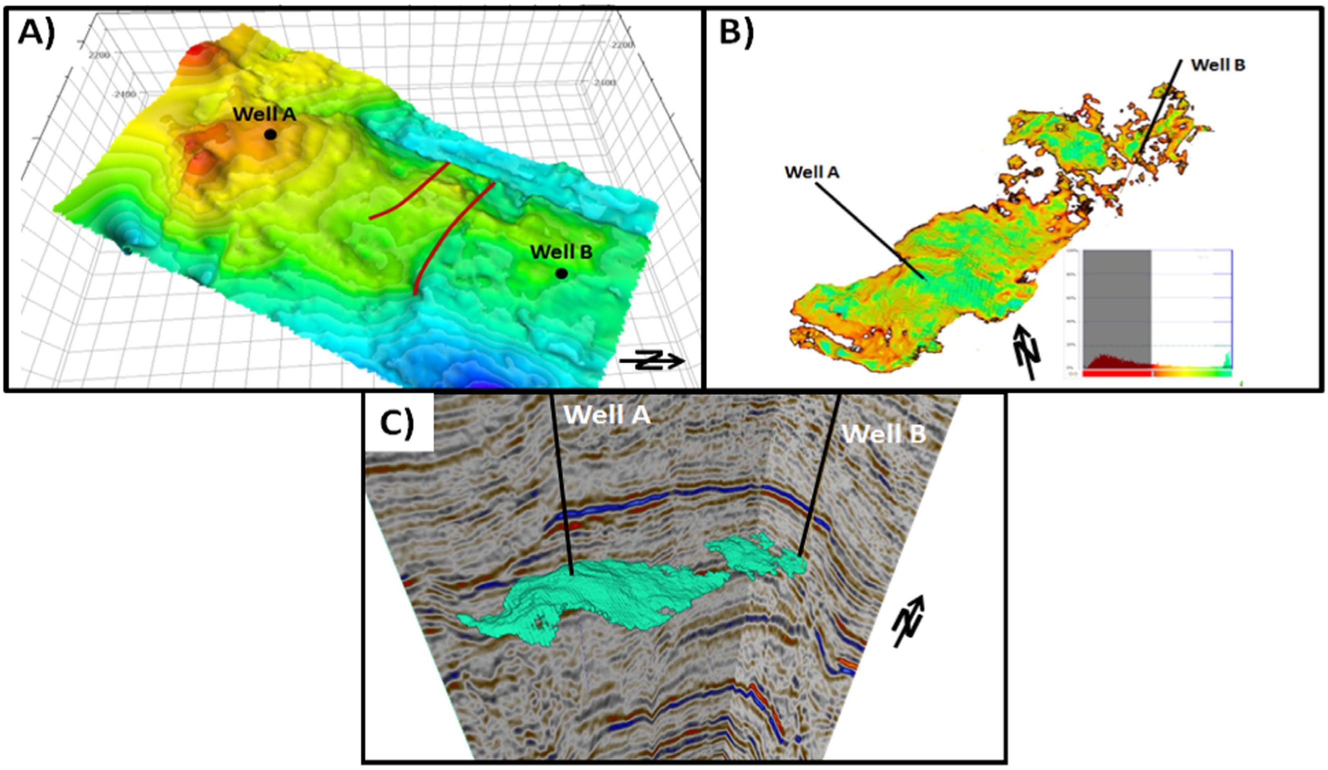

Figure 6. Seismic-geophysical visualization of the two identified carbonate reservoirs. (A) Albian surface structural map (the same map shows the top of phase 3 and the base of phase 4). At this structural map, the two carbonate shoals are separated by the fault system highlighted by the red lines, and each reservoir is characterized by wells A and B, respectively. (B) Geobody extracted from the sweetness volumetric attribute with opacity and transparence illumination that shows the discontinuous carbonate reservoir rock distribution. (C) The main carbonate reservoir distribution (phase 4), verified at wells A and B, are shown here; the main extracted geobody from the seismic data is observed here.

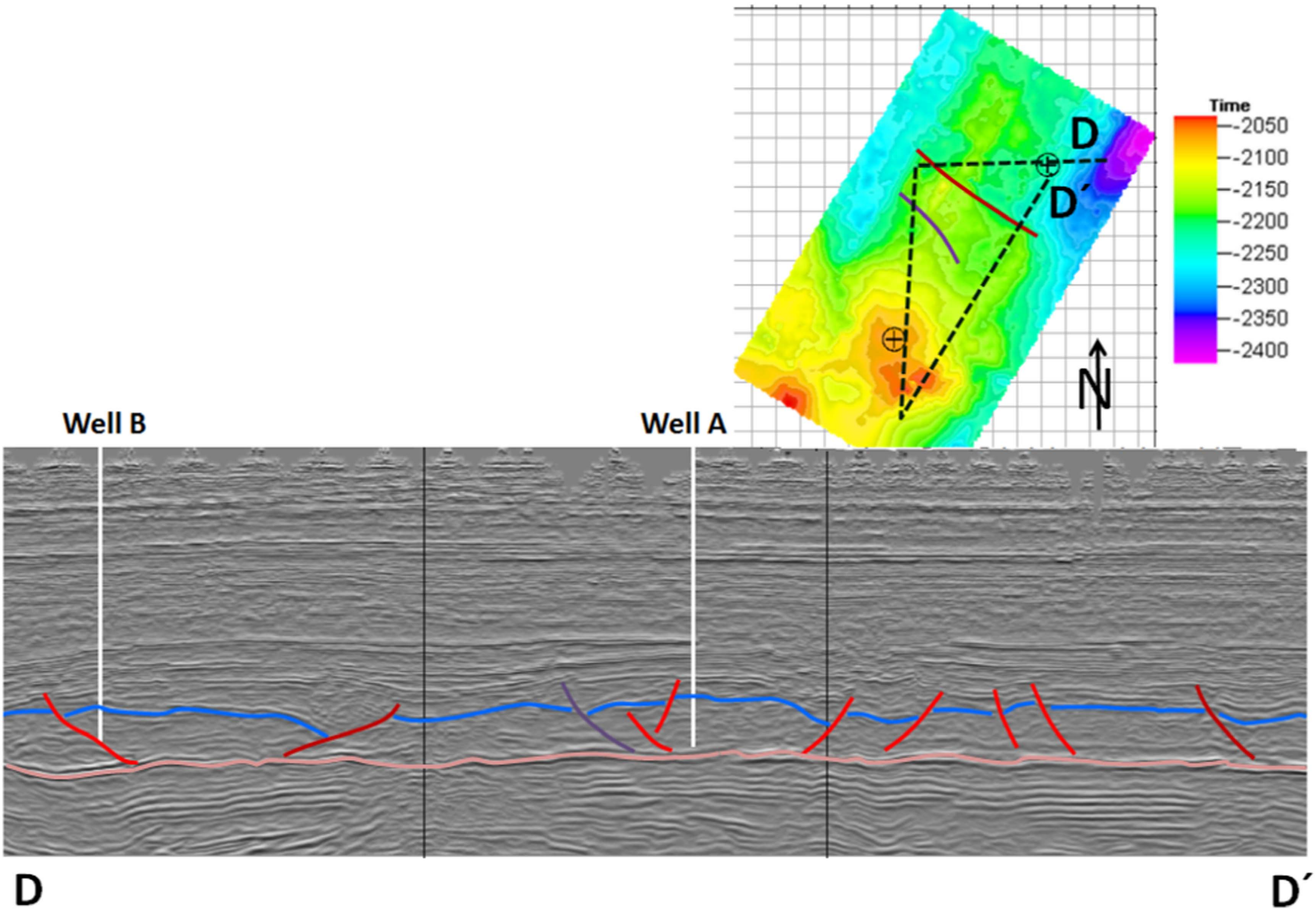

Figure 7. Seismic section D–D' showing a structural high and a horst structure limited by two main faults presented in the map (dark red and violet faults). These two faults divide the carbonate shoal in the north and south regions, and both regions contain hydrocarbon production from wells A and B, respectively. The dip slip of the dark red fault is approximately 150 m (80 ms), and it is the limit of the hanging-wall (lower block) at the north of the studied area.

deposited in shallow marine environment of high to moderate energy. The lithological composition is mainly grainstone and packstone, formed by oncoids, ooids, peloids and bioclasts controlled by the environmental conditions, according to the description shown in table 1 (Spadini *et al* 1988, Favoreto 2014, Favoreto *et al* 2016).

The Outeiro formation is formed from fine grained carbonates interbedded by marls and shale deposited in response to sea level rise. It is composed of highly micrite rocks (mudstone/wackestone) and particularly by characteristic fossils from open sea water (*P. sphaerica*, *Favusella whashitensis*, among others), which confirms a significant marine transgression in this phase (Dias-Brito 1982, Favoreto 2014, Favoreto *et al* 2016).

2. Methods and material

We aim to characterize the paleo-geographic evolution of carbonate bank oil production by the integration of geological and geophysical data. Through the research, techniques related to petrographic analysis, paleogeography diagram blocks and seismic attributes maps were applied.

As such, the spatial distribution and paleo-sedimentary environment evolution of the different geological facies were conducted based on the following features: (1) type of grain; (2) micrite occurrence; (3) diagenetic features; (4) fossiliferous content; (5) vertical stacking pattern; and (6) well stratigraphic correlation.

Favoreto *et al* (2016) described approximately 400 m of cores (the upper part of the Quissama reservoir and the lower part of the Outeiro formation) from four wells provided by Petrobras for this analysis; as a result, the diagenetic facies and fossiliferous content were defined in order to characterize the different depositional phases.

The obtained geological facies were extrapolated at the region, firstly for non-cored wells by rock–wirelog correlation, and after, by the use of seismic attributes in a quantitative and geologically controlled way.

The phase of extrapolation to non-cored wells includes the elaboration of numerical models by electrofacies definition (EFAC). This method enables us to build a lithological model from non-cored wells based on a non-supervised neural network (Rogers *et al* 1992) that represents the relationship between a rock's physical properties and its own signal at the wire logs.

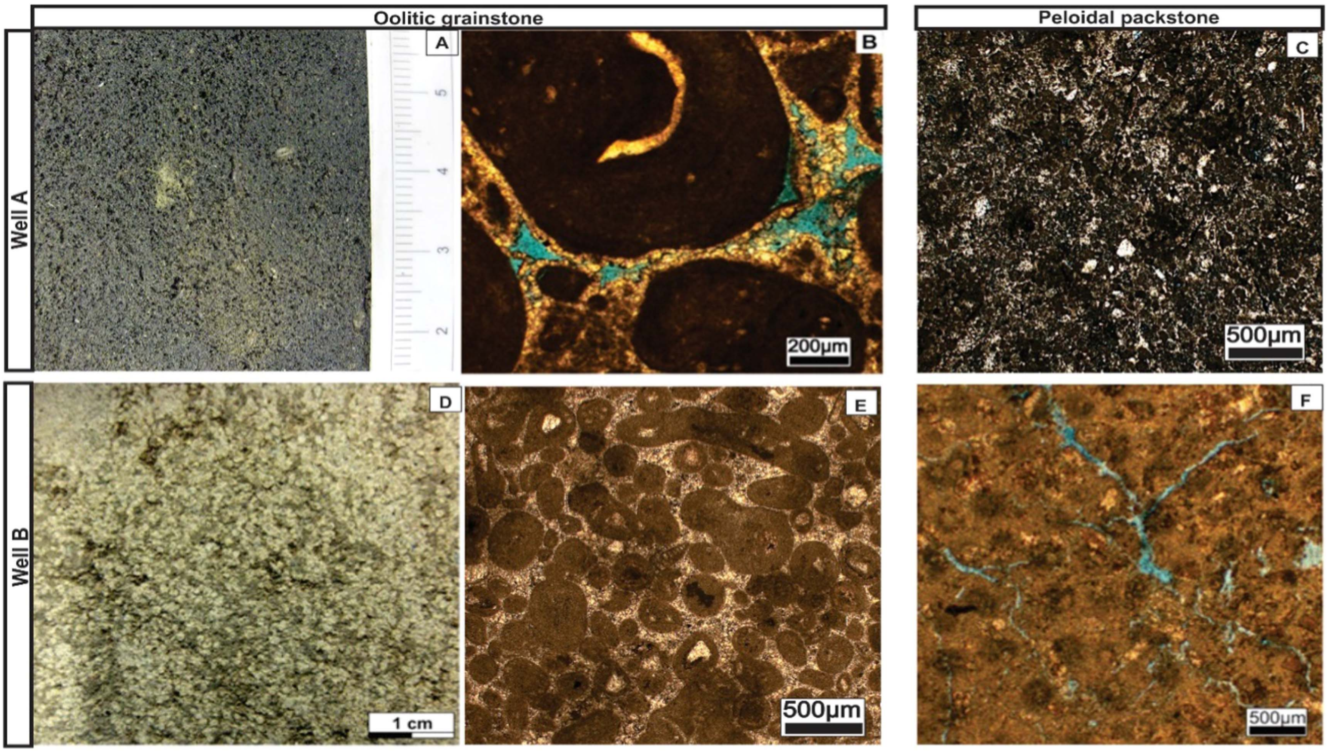

Figure 8. The difference between grainstone oolitic facies and peloidal packstone observed at wells A and B. (A) Oolitic grainstone (core sample) with high porosity and a dark color due to petroleum impregnation; (B) photomicrographs of sample A, with prismatic fringe with compaction; (C) peloidal packstone with fine mosaic cementation and intergranular pores; (D) oolitic grainstone, core detail, showing a mottled aspect (cement and oil distribution); (E) well-sorted oolitic grainstone, showing partial to total micritization; (F) packstone-peloidal, with intense fracturing responsible for the oil production at the southern region.

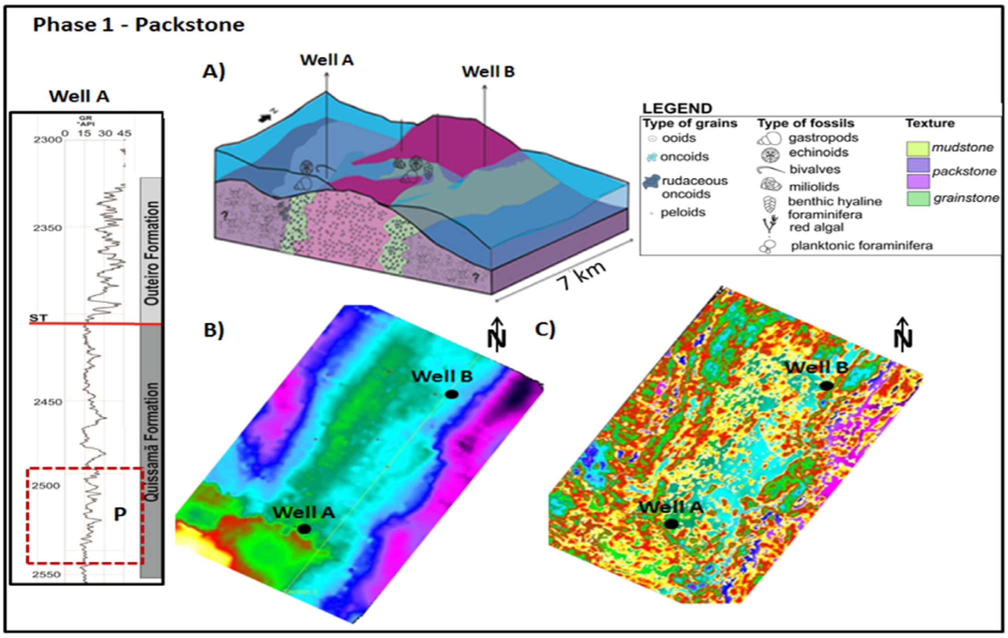

Figure 9. Geological and geophysical characterization of the facies packstone representative of the carbonatic bank. (A) Substrate and diagram block of the paleo-environment for phase 1; (B) contour structural map of the top of phase 1 (the hot colors represent structural highs and the cool colors relate to structural lows; (C) seismic attribute map of maximum negative amplitude representing the heterogeneities of the packstone facies at the substrate of the analyzed carbonate bank.

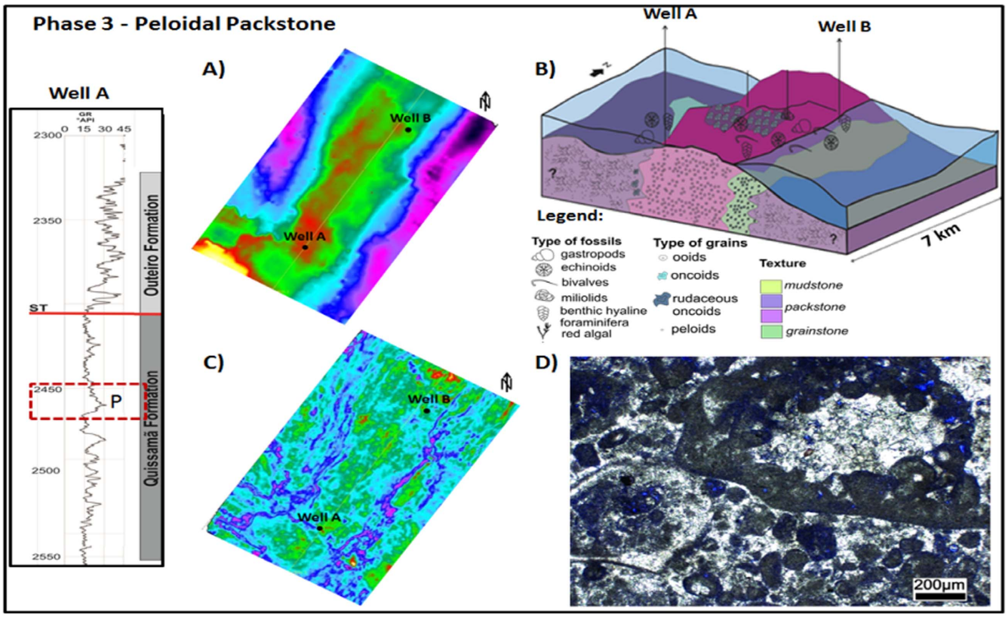

Figure 10. Geological and geophysical characterization of the carbonatic shoal evolution (facies peloidal/packstone). (A) Contour structural map of the depositional sequence 3 (the hot colors represent structural highs and the cool colors relate to structural lows; (B) diagram block of the paleo-faciological condition of this region; (C) seismic attribute map of maximum negative amplitude showing the distribution of the peloidal packstone facies, represented by green anomalies; (D) photomicrograph of peloidal packstone facies representative of the stratigraphic interval shown at the well profile at the left of the global figure at well A.

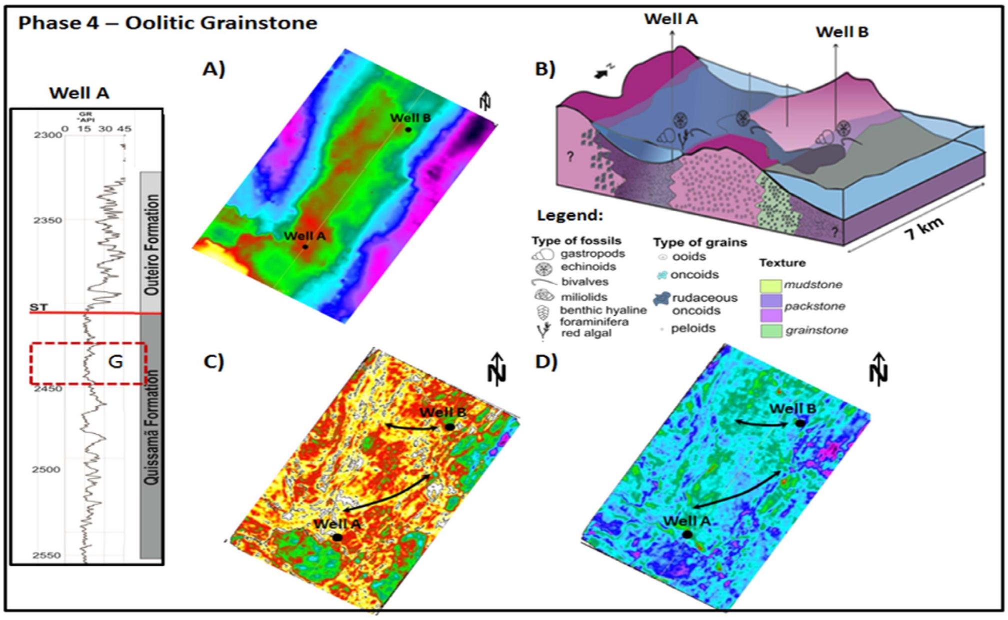

Figure 11. Geological and geophysical characterization of the main reservoir (oolitic grainstone). (A) Contour structural map of phase 4 (the hot colors represent structural highs and the cool colors relate to structural lows; (B) diagram block of the paleo faciological condition at phase 4; (C) seismic attribute map of maximum negative amplitude representing the heterogeneities of grainstone facies with the paleo-channels that connect the open sea shelf to the restricted circulation shelf (the paleo-channels are represented by the yellow anomaly and black arrows); (D) seismic attribute map of the main amplitude showing the grainstone facies heterogeneities. The green anomaly was considered to be the best reservoir facies.

The EFAC determination directly addressed the relationship between the core's facies and wire log's facies that led the process of the facies's definition on 24 non-cored wells in order to generate maps of faciological distribution (Sarzenki and Toledo 1990, Castro 1998, Sombra 2005) for the different stratigraphic intervals of the Quissama and Outeiro formations.

The graphical signal in the electrical profiles (wirelogs) was visualized from the described core's facie. The gamma ray and sonic (DT) were the wire logs that better presented

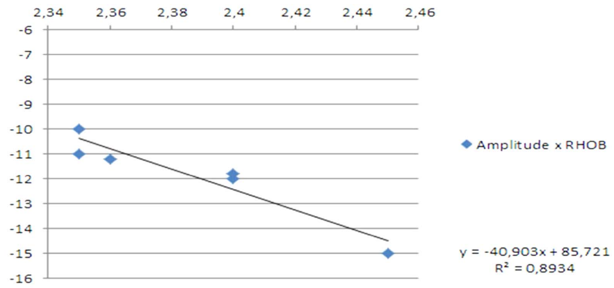

Figure 12. Cross-plot of the correlation of amplitude versus rock density (reservoir quality) showing a linear relationship between the seismic attribute and the carbonate rock type effective reservoir.

control of the EFAC classification, and other profiles, such as neutron porosity (NPHI) and density (RHOB) helped in the classification process. Consequently, the correlation coefficient obtained from the EFAC definition and the core's facies was higher than 60%–70%.

The second phase of the facies extrapolation relates to geophysical analysis, where the upscaling rock–wirelog–seismic is performed. After the identification of each reference reflector (stratigraphic level/phase) at the seismic volume, each one was interpreted, resulting in four related surfaces of a top and base depositional interest interval sampled at the Albian.

After these surface mappings, geological profiles were built with the objective of identifying the tectonic evolution of each sedimentary sequence (phase), and for each surface, seismic attribute maps were calculated.

The amplitude anomalies were determined by the use of the calculated attribute maps (*root mean square*, *mean amplitude*, *average amplitude*, and *energy*, among others) for the top of each interpreted sequence and at the intra-sequence levels.

By applying the seismic attribute maps, the described geological facies were statistically evaluated using correlation cross-plots of amplitude anomaly versus facies (figure 4), in order to obtain a characterization of facies distribution in the field of study. When the rock attribute value aligns with the value of the seismic attribute, the interpretation is that it is possible to predict a specific rock property using seismic attribute maps; however, if the graphic shows a high dispersion (without a linear correlation), it means that the selected rock property is not represented by the attribute map.

Paleogeography maps for each evolutionary phase were created and defined based on the data integration (rock/seismic); as previously mentioned, the tectonic-stratigraphic evolution of the carbonate bank was well represented in geological sections and confirmed by evolution considerations mentioned in this study.

3. Results

3.1. Paleogeography of a carbonate bank

The carbonate bank part of this research evolved in the rift sequence's paleo-high from the Aptian age. This geological feature was visualized in the SW region, as shown in the maps in figure 5. The mean carbonate structure was conditioned by the basement's paleo-geography, followed by halokinetic deformation that configures structures like rollovers in the west (see this geometry at the top of the Macae Group seismic interpretation in figure 5), and it also determines an internal fault's own system of rheology of the carbonate shoal with a regional ductal compensation at the evaporator sequence (Retiro formation, Aptian top).

At the seismic line in figure 5, the upper rift's sequence (between the green and red horizons) is observed, and at the SE portion, the horst shows a dip slip of approximately 380 m. The structural deformation is significantly influenced by basement highs and structural lows (see the contour structural map at the right of the seismic line (figure 5)).

The Aptian structural configuration has provided almost simultaneous development of two carbonate banks in the Albian age—a fact which was verified with seismic interpretation, and visualized at the opacity and transparency volumetric seismic attributes at the sweetness cube, a seismic attribute that allows the lateral continuity of the carbonate reservoir (figure 6), as defined by Vincentelli *et al* (2014). The substrate is interpreted as approximately the same for both banks, but with a geological division caused by a normal fault system observed from the basement, with the location parallel to the conjugate's deformation system at the Campos Basin in the main direction of NW–SE. This fault system separates the footwall (the high block) of the hanging wall (low structural block) located at the north portion of the evaluated area. The dip slip between the blocks was measured at 150 m (figure 7, phase 1). It was also observed that this fault system was active along the entire phases of the carbonate bank evolution, therefore showing that these two main structural features determine the variance distribution of oil production and petro physical properties.

Following this logic, when comparing the north and south reservoirs, a significant difference is evident between the diagenetic features at the oolitic grainstone and packstones facies. In the north, the rocks showed a prismatic fringe and open framework during eodiagenesis (figures 8(A) and (B)), associated with quartz and detrital feldspar, and the porosity primary rock was preserved. As a result, the reservoir shows high porosity ($\sim$30%) and permeability ($\sim$85 mD) representing a good reservoir. The packstone facies shows less thickness than the south reservoir (<20 m) and is always associated with ooids, which indicates the possibility of reworking grains by storm waves (Favoreto *et al* 2016).

Unlike the north reservoir, the diagenesis that occurs in the south reservoir shows complete cementation. The meteoric-phreatic diagenesis is represented by dissolution (enlarging the intergranular pores and creating moldic porosity) and precipitation of equigranular mosaic cement (figures 8(D) and (E)) (Favoreto *et al* 2016). Although the primary porosity is not preserved and there is low pore connection (low permeability), this reservoir shows porosity channels (in enlarged fractures) influenced by the main fault that contains this field. This condition is favorable for oil field production from fractures in packstone facies. The packstones packages are thicker than 30 m, and are composed of peloids, a micritic matrix, mosaic cementation and porosity along the channels (fractures).

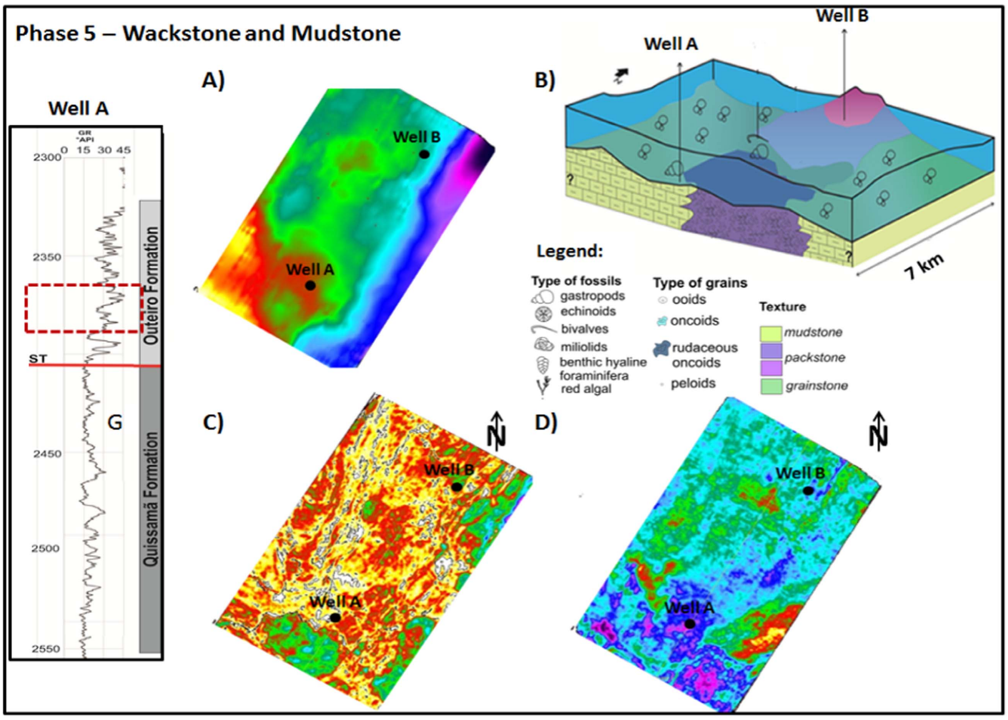

Figure 13. Characterization of the facies wackestone and bioclastic's mudstone representative of the Outeiro formation. (A) Contour structural map of the depositional sequence 5 (the hot colors represent structural highs and the cool colors relate to structural lows; (B) diagram block of the paleo-faciological condition at phase 5; (C) seismic attribute map of maximum negative amplitude representing the heterogeneities of the wackestone and mudstone facies, with green and red anomalies; (D) seismic attribute map (amplitude) showing the heterogeneities for the bioclastic mudstone and wackestone facies, with grainstone development at regions with high energies at the deposition ages, shown by green and red anomalies.

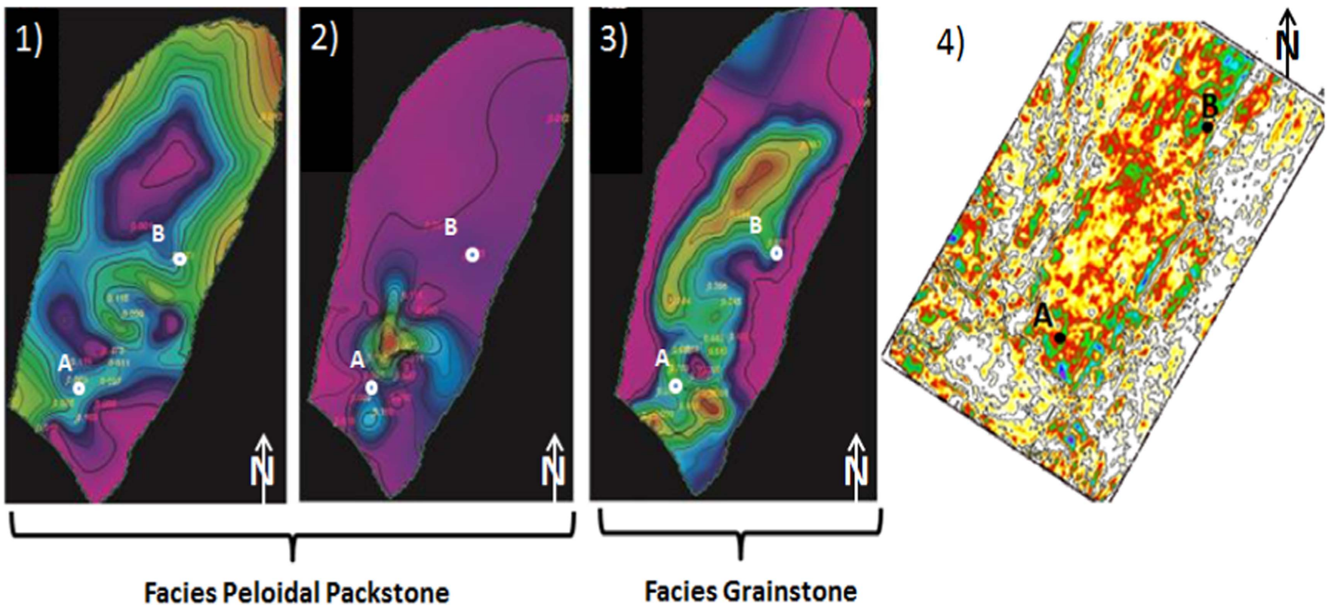

Figure 14. Proportion facies maps at phase 2 (secondary reservoir—1, 2 and 3); maximum negative amplitude map showing the lateral continuity of (phases 2–4), confirmed by the grainstone proportion facies map (3).

3.2. Carbonate bank tectonic-stratigraphic evolution

The paleo-environmental conditions were interpreted based on geological characteristics, such as grain selection, rare bioturbation and bioclast, observed mainly at the grainstone facie. The stratigraphic correlation showed that the carbonate bank thickness varies laterally and is controlled by the shoal evolution, implying a certain mobility of its banks. At the portion of the deeper bank, ooids and oncoids are present, and

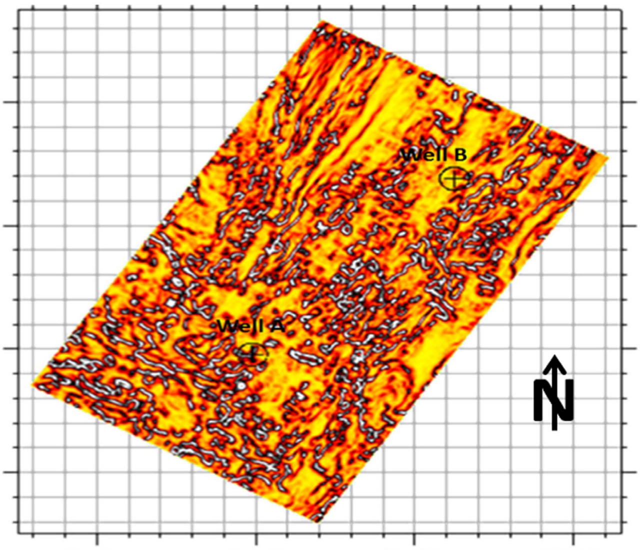

Figure 15. Seismic attribute map of the dip calculated at the main reservoir level of 2475 m in well A. The map shows the stratigraphic level highly fractured at the south portion and less fractured at the north. This result is confirmed when the core is observed at the same level for well B.

at the marginal portions, micrite and rudaceous oncoids have been identified.

At the main carbonate bank, the older facies corresponds to packstone (phase 1, figure 9), which represents the carbonate shoal substrate. The next phase (2) shows the development of grainstone facie, followed by what is considered to be the main depositional sequence (phase 3) representative of the geological evolution.

Along the shoal's evolutionary history, it was observed that phase 3 demonstrates a larger development of its depositional sequence (figure 10). At this phase, the peloidal packstone facies (with rudaceous oncoids) are present in a preserved environment created by barriers or local lows adjacent to the bank (mini-basins). The previous condition was confirmed by the structural map where its main azimuth NE-SW is observed, and it shows the structural lows in the same direction (figure 10(a)). The relative sea level oscillation caused the shoal's subaerial exposition, which generated a meteoric vadose diagenetic environment followed by the generation of partial dissolution represented by moldic porosity (figure 10(b)).

Considering the mean amplitude seismic attribute map (figure 10(C)), it is possible to verify the internal carbonate reservoir heterogeneity caused by the diagenesis development. The seismic anomalies shown in green are mainly modified by blue and red anomalies, a fact that could indicate regions with more (green regions) and less diagenesis (blue and red regions), respectively.

The preservation of the original reservoir facies (grainstone) at the north portion of the block (well B) could be associated with the evidence that this block is located at the structural high and over the oil-water contact.

At this peloidal packstone phase (3), a carbonate bank is confirmed with the azimuth of NE–SW in the contour structural map (figure 10(a)) as well as at the seismic attribute map (figure 10(c)), with an extension of approximately 6 km, showing a thick package of grainstone (up to 30 m thick) at the NE portion. At this location, an abundance of quartz is also observed (usually ooid's nucleus), mica (especially biotite) and potassium feldspar; as a consequence, low energy deposits are thinner and rare. The lateral variation at the carbonate bank may reflect the proximity of Sao Tome Cape at the NE, or any local structural high of this basin.

The rising sea level cycles were the key to determining each reservoir configuration because some regions of the carbonate bank were removed and formed channels that connected the open sea shelf with the restricted circulation shelf, as verified by the attribute map in figure 11 which shows the depositional sequence 4 or phase 4. The amplitude anomalies observed in the mean amplitude and maximum negative amplitude maps clearly show the channels that allow the circulation of marine currents.

At the main amplitude attribute map (figure 11(D)), it is possible to observe higher seismic heterogeneities associated with reservoir facies (green seismic facies), and it was interpreted that this was directly related to the reservoir quality, as verified at the correlation cross plot of figure 12. In the same way, at the maximum negative amplitude map (figure 11(C)), the yellow and red anomalies represent the grainstone facies of Quissama formation.

Above sequence 4, representing the top of the Quissama formation, a marine transgression at the Outeiro formation occurs (sequence 5) characterized by facies like bioclastic wackestone, mudstone and bioclastic's peloidal wackestone, interbedded by marls. These facies are rich in pithonelids, radiolarians and *F. washitensis*, and represent the open sea conditions. The marl presence indicates geological events with higher terrigenous inputs to the basin, and the presence of glauconite indicates less sediment contribution and anoxic conditions.

In summary, the paleogeographic condition of phase 5, represented by mudstones of the Outeiro formation (figure 13), was not uniform along the oil field. At the southern region, the sea level rise creates paleo-environmental conditions that do not support high energy conditions; therefore it is not possible to provide the carbonate bank evolution. At the north position (well B), the primary porosity was maintained because the structural conditions were favorable to the reservoir deposition (grainstone verified at the well) at the structural high of the carbonate platform.

3.3. Qualitative analysis of facies proportion and seismic attribute maps

When the attribute amplitude maps and facies proportion maps are compared, with each identified phase (depositional sequence) elaborated, it is possible to qualitatively verify that the seismic attribute maps of the maximum negative amplitude of phase 2 (figure 14, first recognized reservoir phase) confirms the presence of grainstone facies, highly homogeneous and showing low diagenesis. This, although thin (approximately 15 m), is highly fractured at the southern

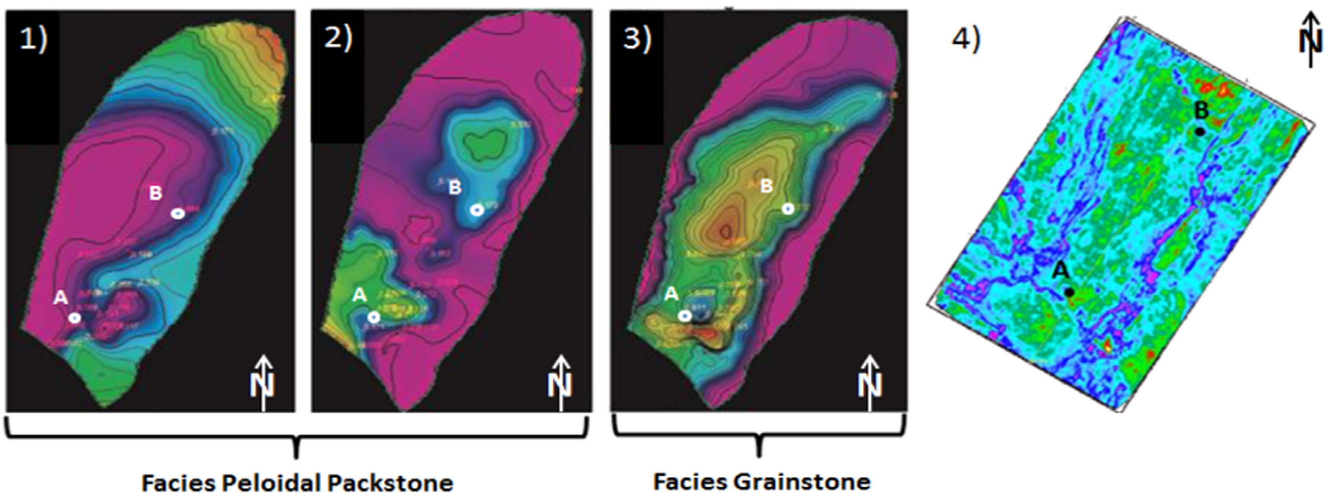

Figure 16. Proportion facies maps of phase 3. Map of mean amplitude generated by seismic attributes. It was observed that at this stratigraphic level, the attribute maps do not distinguish between grainstone and packstone facies.

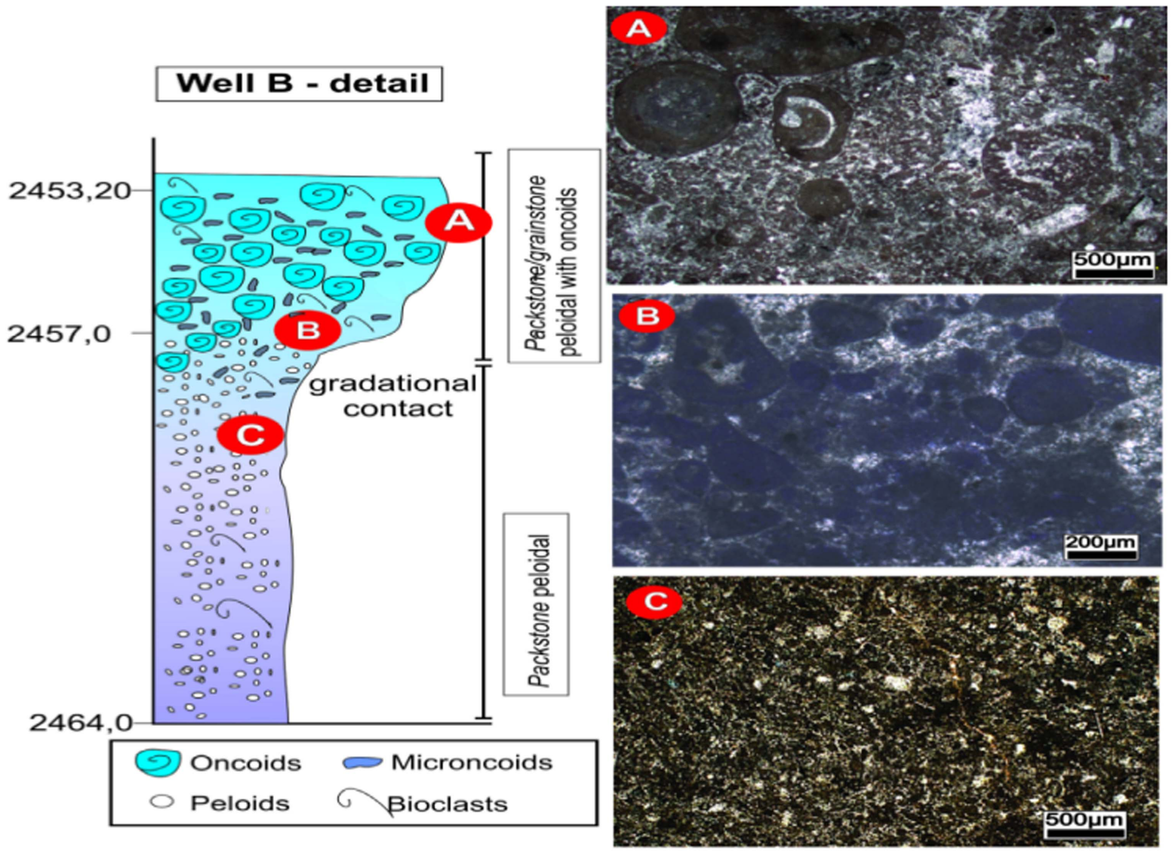

Figure 17. Detail at well B. The intense contact between peloidal packstone and packstone/grainstone facies with oncoiids. The photomicrographs show the gradual transition from ona facie to another, with an important decrease of micrite at the top. In (A) peloidal packstone/grainstone with oncoids—cemented. Micritic oncoids, that could contain gastropods and agglutinated foraminifera inside its nucleous; in (B) peloidal packstone (transition)—a micro-peloidal matrix is observed, micritic oncoids and peloids; (C) peloidal packstone, cemented, formed mainly by peloids.

portion, as verified by the core well data and at the variance seismic attribute map (figure 15).

It was estimated that this fracture system at the southern region is associated with a main fault that limits the evaluated oil field with its southeastern neighborhood oil field. It is important to mention that at the core of well A, a higher fracturing interval of 2475.0–2418.5 m is verified.

The mean amplitude map (seismic attribute) of the third phase (figure 16) confirms the presence of a well-defined central body (green anomaly), with the main direction of

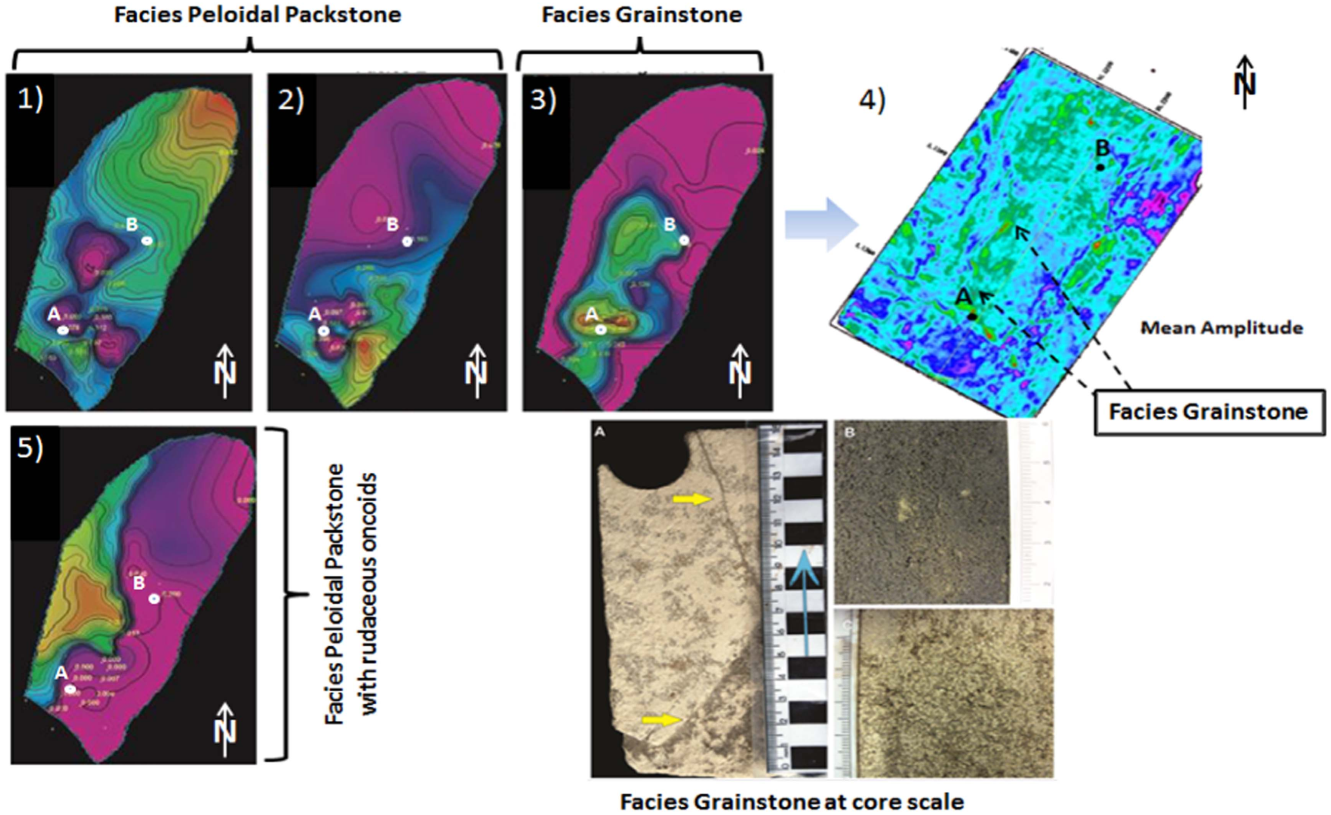

Figure 18. Proportion facies maps of phase 4: map of mean amplitude generated by seismic attributes, and reservoir rock in core scale. As a qualitative interpretation, the green geophysical facie represents the grainstone facie.

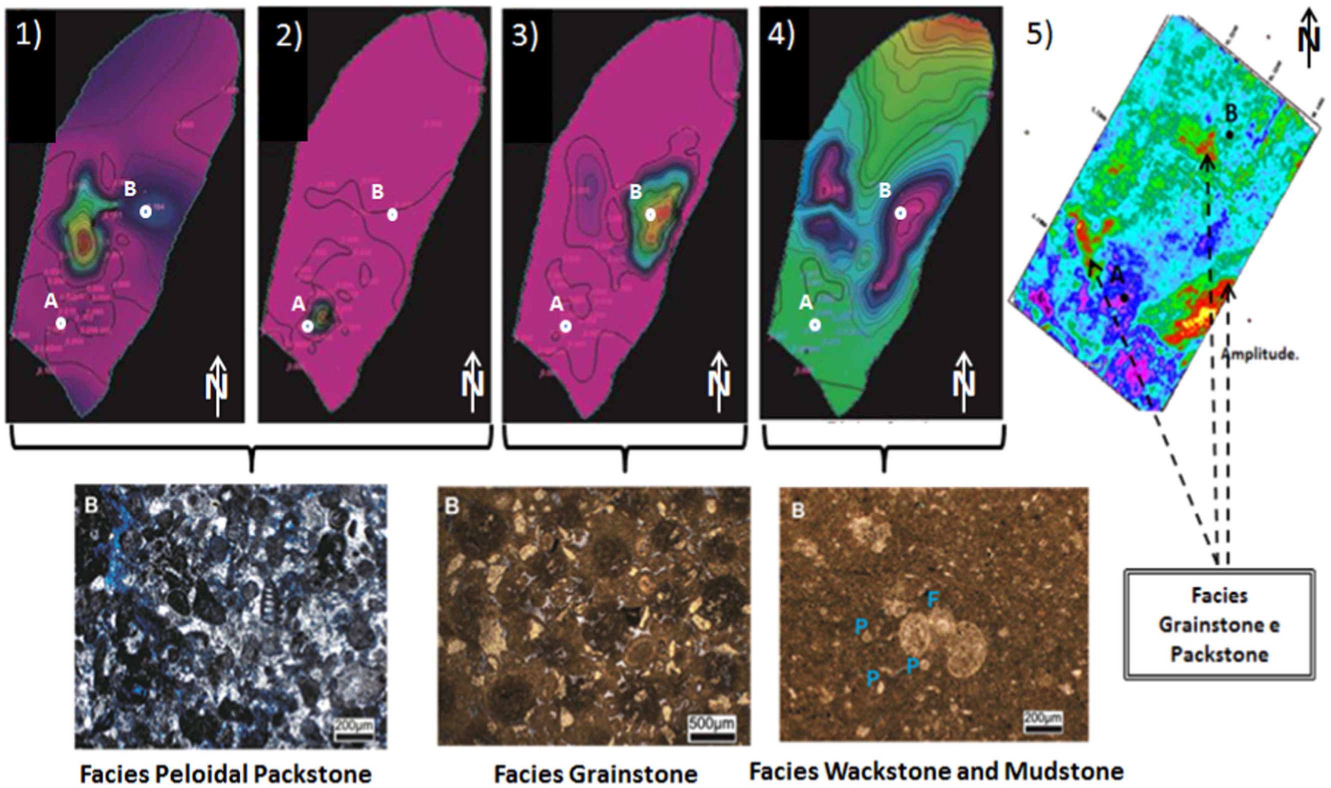

Figure 19. Proportion facies maps of phase 5 (1–4) and amplitude seismic attribute map (5). In the final one (5), it can be seen that the Outeiro's formation distribution is not homogenous, with lateral changes to grainstone and packstone facies, as exemplified at the thin section images.

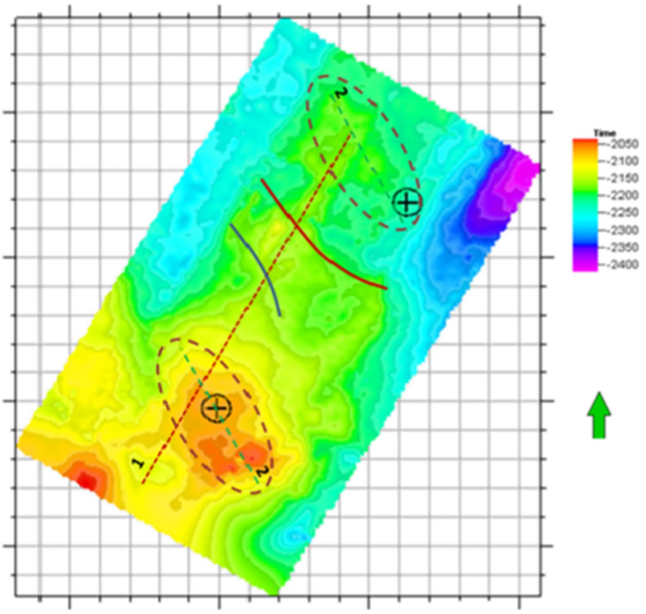

Figure 20. Structural map at the top of the Macae Group showing the two structural paleo-highs of the carbonatic bank defined for the regions at wells A and B, both separated by a normal fault system. The red fault shows a sinistral movement, which represents a left movement of the north blocks when compared with the south blocks. This relative movement is associated with the start of halokinetic deformation.

NE–SW, which matches the main geological feature related to grainstone facies distribution at the proportion map (figure 16(3)).

At the lateral region of the main geological body (carbonate shoal), a seismic anomaly discontinuity was verified that could be because, at this depositional sequence, the attribute maps do not distinguish the difference between peloidal packstone and grainstones facies, possibly caused by the gradational contact between both facies (figure 17).

The depositional sequence before the previous one (phase 4) represents the main carbonate reservoir (grainstone facies), approximately 40 m thick and a porosity of up to 18%, which is recognized as a less homogeneous reservoir than phase 2. Good homogeneity is confirmed at the mean amplitude map (figure 18(4)); however, two main NW–SE trends are clear. These two trends characterize two carbonate banks, not interconnected, as shown in the grainstone proportion map in figure 18(3). The packstone facies appear to be overestimated on its proportion map (figures 18(1) and (2)), when compared to the mean amplitude and maximum negative amplitude maps (figure 18(4)); a higher heterogeneity of the grainstone's facies and some anomalies at the maximum negative amplitude map (green) could be caused by the presence of peloidal packstone.

Phase 5 corresponds to the facies distribution of the Outeiro formation (violet and blue anomalies in the map of figure 19(4)), and the presence and distribution of grainstone and packstone facies visualized and localized mainly in three areas (green and red anomalies, figure 19(5)) was observed; these last facies were not characterized from core data because this location was not drilled by any well, but the facies proportion maps indicate its presence (figure 19: maps 1, 2, 3).

4. Discussion of results

The structural map at the top of the Macae Group (figure 20) represents the geometry of the Quissama reservoir's sequence. At the top of the map, a homoclinal structure extends towards NE–SW, as indicated by the red line (number 1) in figure 20. However, a detailed paleo-geographic analysis performed at the Albian sequence identified that the oil producing structures at the north and south, highlighted by the red ellipse in the same figure, present the main axis of the carbonate bank evolution in the NW–SE direction, identified by the green line (number 2). Therefore, the evolution of the two carbonate banks along a pre-existing basement paleo-high with a fault system parallel to the rift direction (NE–SW) relating to the Gondwana opening is observed—a process which divides the African and South American continents. Moreover, the presence of both carbonate banks was determined by a normal fault system relating to the initial stages of halokinetic deformation, which pre-determines the existence of structural highs formed by listric faults in the conjugate direction (NW-SE) of the main basin's fault system. The only two pre-existing highs formed the oil producing reservoirs associated with wells A and B, because both were held in high-energy conditions.

Despite the fact that the cemented depositional facies, observed at the SW region, are not favorable for an oil reservoir at this portion of the field, the fracturing system visualized in figure 21 was intense and allowed oil accumulation in the area of well B (Favoreto 2014). When observing the attribute maps of the main reservoir (phase 4, figure 11) that represent the reservoir quality (as verified at the correlation cross-plot), the red anomalies indicate the best reservoir quality in the north, center and south of the studied area. These anomalies reflect the distinctive paleo-geographic conditions identified for these areas; this diversity might explain the difference observed between the hydrocarbon production curves associated with each of these regions.

Finally, it is possible to confirm that the existence of these hydrocarbon accumulations are directly related to the dominant tectonic-stratigraphic system at this basin portion over the Albian age. Due to high-energy conditions observed at its main reservoir (phase 4), the presence of the structural paleo-highs formed by the halokinetic fault system at this period of time were made possible, and the main bank's growth direction (NW-SE) was controlled by the same factor. Even the presence of a normal fault at the north portion, with sinistral movements and a dip slip of approximately 260 m, allowed greater depth conditions during the Albian sequence at well B when compared with well A, avoiding subaerial exposures of the block. Therefore, its initial diagenetic conditions were held in a low degree when compared with well A.

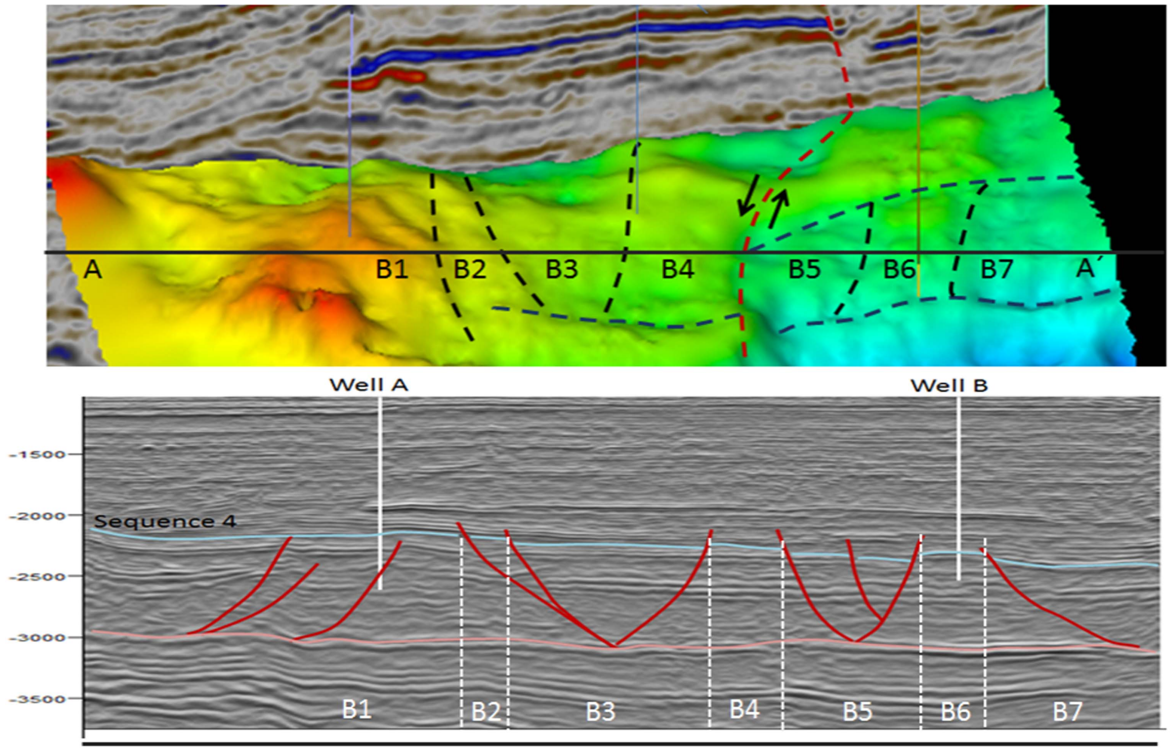

Figure 21. Geological geometry of the paleo-structural situation of phase 4, where the carbonatic reservoirs evolved as the main hydrocarbon reservoirs.

5. Conclusion

The tectonic-stratigraphic conditions related to the evolution of the main carbonate oil reservoirs were determined for the reservoir facies (grainstone) distribution. As a result, it is confirmed that the presence of basement paleo-highs, in the same direction as the main rift structures of the Campos basin, generate favorable conditions for the carbonate bank evolution. In addition, the deposition of the effective reservoir facies depends on the high energy conditions created by adjacent mini-basins to the main bank. These conditions are favorable for the development of packstone facies that originate as the necessary substrate for good reservoir facies (grainstone) deposition. At the studied oil region, only two areas demonstrated the necessary environmental conditions to maintain high energy conditions; these areas evolved over structural highs (horst) associated with an extensional deformation system related to the first halokinetic stages of the basin in a fault system in the antithetic direction (NW–SE) to the main structural rift's deformation system (NE–SW).

The analyzed carbonate bank was subdivided into five phases, described as follows (from bottom to top): (1) the first depositional sequence of the bank was composed mainly of packstone, indicating that the local structural lows adjacent to the main bank are protected from environmental conditions; (2) characterized by the presence of grainstone developed at the structural high; (3) main sequence of a peloidal packstone, with mudstone oncoids; (4) corresponds to the main carbonate reservoir oil production, formed by oolitic grainstone deposited at the top of the carbonate bank—at this phase the rising sea level formed channels that connected the open sea shelf with the restricted circulation shelf; and (5) mudstone and wackestone represents the flooding phase of the system.

Finally, after performing an integrated geological-geophysical analysis in order to better understand the regions of the oil field that actually maintain good reservoir facies, and to explain why they would be present, it is possible to reproduce the evolution of the carbonate bank history using seismic interpretation and seismic attributes, but calibration with well data and thin section information are determinant factors in the understanding of seismic attributes, which are different for each carbonate bank.

Acknowledgments

The authors want to thank Petrobras for allowing access to the dataset and publication of the geological-geophysical results, and UNESPetro/LISG laboratory at UNESP for the facilities in executing the research.

References

Asmus H E 1975 Controle estrutural da deposição mesozoica nas Bacias da margem continental brasileira *Revista Brasileira de Geociências* **5** 160–75

Asmus H E and Guazelli M 1981 Descrição sumária das estruturas da margem continental brasileira e das áreas oceânicas e continentais adjacentes *Projeto Remac* **9** 187–269

Azevedo R L M O 2001 Albiano no Atlântico Sul: estratigrafia, paleoceanografia e relações globais *Tese de Doutorado* Instituto de Geociências, Curso de Pós-Graduação em Geociências, Universidade Federal do Rio Grande do Sul

Azevedo R L M, Gomide J, Viviers M C and Hashimoto A T 1987 Bioestratigrafia do Cretáceo marinho da Bacia de Campos, Brasil *Revista Brasileira de Geociências* **17** 147–53

Cainelli C and Mohriak W U 1998 Geology of Atlantic eastern Brazilian basins *1998 AAPG-Int. Conf. and Exhibition (Rio de Janeiro)* vol 2, p 66

Castro W B M 1998 Correlação rocha-perfil através de regressão logistica *Master's Thesis* Universidade Estadual de Campinas

Chang H K, Kowsmann R O, Figueiredo A M F and Bender A 1992 Tectonics and stratigraphy of the east Brazil rift system: an overview *Tectonophysics* **213** 97–138

Dias-Brito D 1982 Evolução paleoecológica da Bacia de Campos durante a deposição dos calcilutitos, margas e folhelhos da Formação Macaé (Albiano e Cenomaniano) *Boletim Técnico da Petrobras* **2** 84–97

Dias J L, Scarton J C, Esteves F R, Carminatti M and Guardado L R 1990 Aspectos da evolução tectono-sedimentar e a ocorrência de hidrocarbonetos na Bacia de Campos ed G P Raja Gabaglia and E J Milani *(Coords.) Origem e evolução de Bacias Sedimentares* (Rio de Janeiro: Petrobras) pp 333–60

Favoreto J 2014 Modelo deposicional de carbonatos Albianos da Formação Quissama: análise faciológica, diagenética e estratigráfica de um campo de óleo na porção meridional da Bacia de Campos *Dissertação de mestrado* Universidade Estadual 'Julio de Mesquita Filho'

Favoreto J, Rohn R, Lykawa R and Okubo J 2016 Caracterização sedimentológica dos carbonatos Albianos do reservatório Quissama na porção meridional da Bacia de Campos *Revista Geociências* **35** 1–15

Guardado L R, Mello M R, Spadini A R and Brandão J S L 2000 Petroleum system of the Campos Basin, Brazil *AAPG Memoir* **73** 317–24

Guardado L R, Gamboa L A P and Lucchesi C F 1989 Petroleum geology of the Campos Basin, Brazil, a model for a producing Atlantic type basin *Divergent/Passive Margin Basin* (*AAPG Memoir*) ed J C Edwards and P A Santogrossi vol 48 (Tulsa, OK: AAPG) pp 3–79

Mohriak W E, Mello M R, Dewey J F and Maxwell J R 1990 Petroleum geology of the Campos Basin, offshore Brazil *Classic Petroleum Provinces* (*Special Publications*) ed J Brooks vol 50 (London: Geological Society) pp 119–41

Rangel H D, Martins F A L, Esteves F R and Feijó F J 1994 *Bacia de Campos* 8 (Rio de Janeiro: Boletim de Geociências da Petrobras) 203–18

Rogers S J, Fang J H, Karr C L and Stanley D A 1992 Determination of lithology from well logs using a neural networks *Am. Assoc. Pet. Geol. Bull.* **76** 731–9

Sarzenski O J and Toledo J B 1990 *Correlação rocha-perfil: conceitos e aplicação em reservatórios heterogêneos* (Rio de Janeiro: PETROBRAS/DEPEX/SEIDER-SUPCIA)

Sombra C L 2005 *Calibração de Curvas de Perfis com Análises de Laboratório* (Ouro Preto: UFOP)

Spadini A R, Esteves F R, Dias-Brito D, Azevedo R L M and Rodrigues R 1988 The Macaé Formation, Campos basin, Brazil: its evolution in the context of the initial history of the South Atlantic *Revista Brasileira de Geociências* **3** 261–72

Vincentelli C M G, Cáceres S and Uchoa M 2014 Geophysical characterization of Albia Carbonates reservoirs in Brazilian Basins: the sweetness as a toll for carbonate reservoirs definition *Revista Brasileira de Geofísica* **32** 695–705

Winter W R, Jahnert R J and França A B 2007 Bacia de Campos *Boletim de Geociências da Petrobras* **15** 511–29